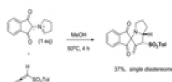


# Phosphorus, Sulfur, and Silicon and the Related Elements



Editor-in-Chief: Martin B. Rudi  
European Editor: Konstantin Karginov

ISSN: (Print) (Online) Journal homepage: <https://www.tandfonline.com/loi/gpss20>

## Synthesis and structural characterization of two rotationally flexible bis(benzoxaphosphole)s

Zakary T. Ekstrom, Arnold L. Rheingold & John D. Protasiewicz

**To cite this article:** Zakary T. Ekstrom, Arnold L. Rheingold & John D. Protasiewicz (2021): Synthesis and structural characterization of two rotationally flexible bis(benzoxaphosphole)s, *Phosphorus, Sulfur, and Silicon and the Related Elements*, DOI: [10.1080/10426507.2021.2011887](https://doi.org/10.1080/10426507.2021.2011887)

**To link to this article:** <https://doi.org/10.1080/10426507.2021.2011887>

 View supplementary material 

---

 Published online: 08 Dec 2021.

---

 Submit your article to this journal 

---

 Article views: 32

---

 View related articles 

---

 View Crossmark data 

## Synthesis and structural characterization of two rotationally flexible bis(benzoxaphosphole)s

Zakary T. Ekstrom<sup>a</sup> , Arnold L. Rheingold<sup>b</sup> , and John D. Protasiewicz<sup>a</sup> 

<sup>a</sup>Department of Chemistry, Case Western Reserve University, Cleveland, OH, USA; <sup>b</sup>Department of Chemistry and Biochemistry, University of California, San Diego, CA, USA

### ABSTRACT

Two bis(benzoxaphosphole)s, 2,2'-diphenyl-7,7'-bibenzo[*d*][1,3]benzoxaphosphole (**1**) and 1,1'-bis(2-benzo[*d*][1,3]oxaphosphole)ferrocene (**2**) have been prepared and fully characterized, including structural characterization by single crystal X-ray diffraction methods. Compound **1** has flexibility about the connecting CC bond as evaluated by DFT calculations. The structure of **2** adopts a configuration in the solid state whereby the two BOP units are held in close proximity, presumably due to  $\pi$ -stacking interactions. Under UV irradiation compound **1** is blue fluorescent with a quantum yield of 18% in THF. Compound **2**, however, displays no significant emission, which is attributed to ferrocene's excited state quenching ability.

### ARTICLE HISTORY

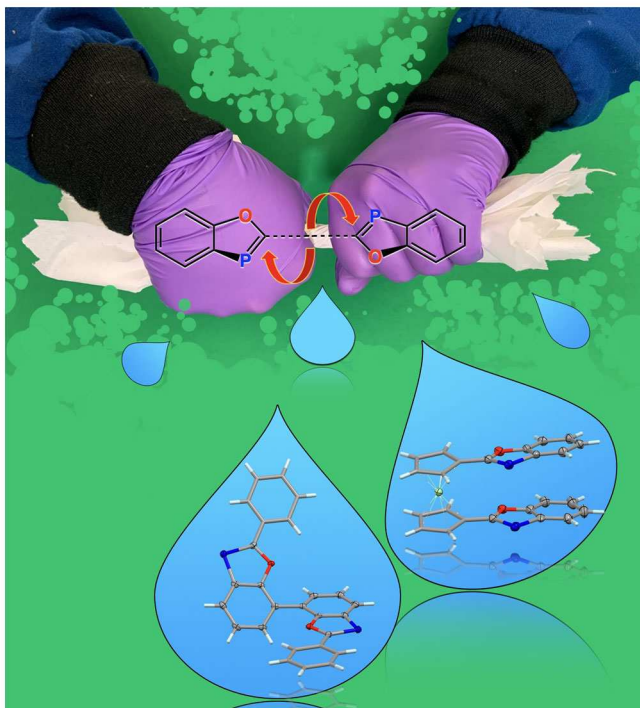
Received 4 November 2021

Accepted 22 November 2021

### KEYWORDS

Benzoxaphosphole; phosphorus; fluorescence; structure; synthesis

### GRAPHICAL ABSTRACT



### Introduction

The development of new  $\pi$ -conjugated organic materials that are electronically active and tunable is a steadily progressing field of study.<sup>[1–6]</sup> Many  $\pi$ -conjugated molecules share a similar core geometry whereby maximal coplanarity and overlaps of  $p\pi$ - $p\pi$  bonds is achieved. Adequate orbital overlap and  $\pi$ -conjugation length allows for the delocalization of electrons

and enhancement of desirable electronic properties such as conductivity and photoluminescence.<sup>[7,8]</sup> Addition of heteroatoms having lone-pairs of electrons and/or accessible  $\sigma^*$  orbitals interacting with  $\pi$ -conjugation pathways has been used as one mechanism to tune HOMO-LUMO bandgaps, allowing access to new optoelectronic behavior.<sup>[5,9]</sup> The exchange of C=C bonds for  $p\pi$ - $p\pi$  P=C bonds along the  $\pi$ -conjugation

**CONTACT** John D. Protasiewicz  [protasiewicz@case.edu](mailto:protasiewicz@case.edu)  Department of Chemistry, Case Western Reserve University, Cleveland, OH 44106, USA.  
This article is dedicated to Francois Mathey, an inspirational pioneer for phosphorus heterocycles.

 Supplemental data for this article can be accessed online at <https://doi.org/10.1080/10426507.2021.2011887>.

© 2021 Taylor & Francis Group, LLC

paths of molecules result in a notable lowering of the LUMO energies and corresponding red-shifted absorptions.<sup>[7,10,11]</sup>

Integration of  $\pi\pi$ - $P=C$  bonds within five- and six-membered heterocycle rings, can, in select cases, afford photoluminescent molecules which have garnered attention as “photo-copies.”<sup>[7,12–17]</sup> Our group provided a detailed study of the first examples of these molecules featuring 2-Ar-1,3-benzoxaphospholes (Figure 1, BOP/PC-1) in 2010.<sup>[14]</sup> 2-Aryl-BOPs display blue fluorescence with quantum yields (QY) ranging from 12% to 60%.<sup>[12,14]</sup>

Several other classes of phosphorous substituted heterocycles that display noteworthy fluorescent properties have been developed (Figure 1). The Noonan group was able to prepare benzothiaphospholes<sup>[13]</sup> (PC-2) and benzobisthiaphospholes<sup>[18]</sup> (PC-3) with QY varying from 1.5% to 5.5% and 0.3% to 5.4% for PC-2 and PC-3, respectively. Air tolerant 9-phosphaanthracenes (PC-4) developed by Ito and Mikami displayed QY of 0.1%–13%.<sup>[15]</sup> A series of fluorescent 2-pyridyltriazaphospholes developed by Mueller, Hissler and Nyulászi<sup>[16]</sup> (PC-5) achieved QY’s of 11%–12%. More recently Nagahora and coworkers developed p-

henylenephosphinines (PC-6) with fluorescence QY in solution and PMMA films ranging from 1.0% to 54%.<sup>[17]</sup>

Our group has also developed luminescent compounds having two or more BOPs linked by conjugated units (BBOP and bisBOP, Figure 1).<sup>[19]</sup> This work demonstrated that the color of emission depended on the nature of the intervening  $\pi$ -conjugated linker. This work has inspired us to examine the impact of imposing additional geometric constraints between two BOP motifs, independently of  $\pi$ -conjugation. In this work we have thus explored the synthesis and characterization of two rotationally flexible bisBOPs using the readily available precursors 2,2'-biphenol and 1,1'-ferrocenedicarboxylic acid.

## Results and discussion

### Syntheses

The synthesis of most BOP-type molecules requires suitable *ortho*-hydroxy phenyl phosphines. 2,2'-Diphenyl-7,7'-bibenzozo[*d*][1,3]benzoxaphosphole **1** was prepared starting from commercially available 2,2'-biphenol in three steps, as shown in Scheme 1. First, reaction of commercially available 2,2'-biphenol with two equivalents of diethyl chlorophosphate with a slight excess of triethyl amine afford the tetraethyl diphosphosphate (**1a**) in 50% yield.<sup>[20]</sup> Compound **1a** was then subjected to an anionic *phospha*-Fries rearrangement cleanly yielding the tetraethyl bis(phosphonate) (**1b**) in 94% yield. Reduction of **1b** in anhydrous diethyl ether with lithium aluminum hydride gives the 3,3'-diphosphino-2,2'-biphenol (**1c**) in 86% yield as an air-stable white solid. The  $^{31}\text{P}$  NMR of **1c** is shifted downfield compared to 2-phosphinophenol ( $\delta = 145.2$  ppm vs.  $\delta = 154.1$  ppm). As expected for a primary phosphine, the resonance is a triplet with a coupling constant of  $J = 206.5$  Hz (e.g., 2-phosphinophenol,  $J = 205.3$  Hz).

Refluxing **1c** in toluene with two equivalents of benzoyl chloride under anaerobic conditions affords **1** (Scheme 1B)

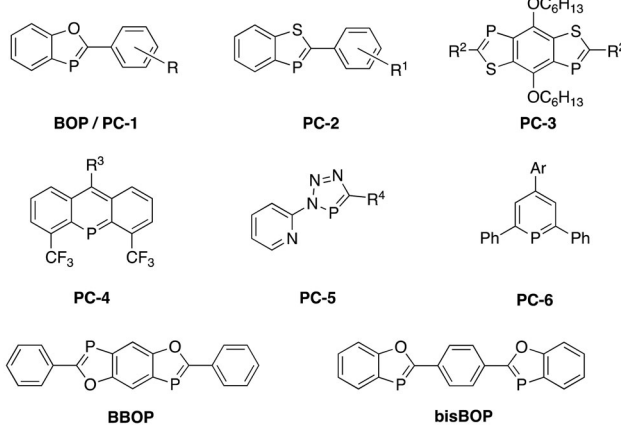
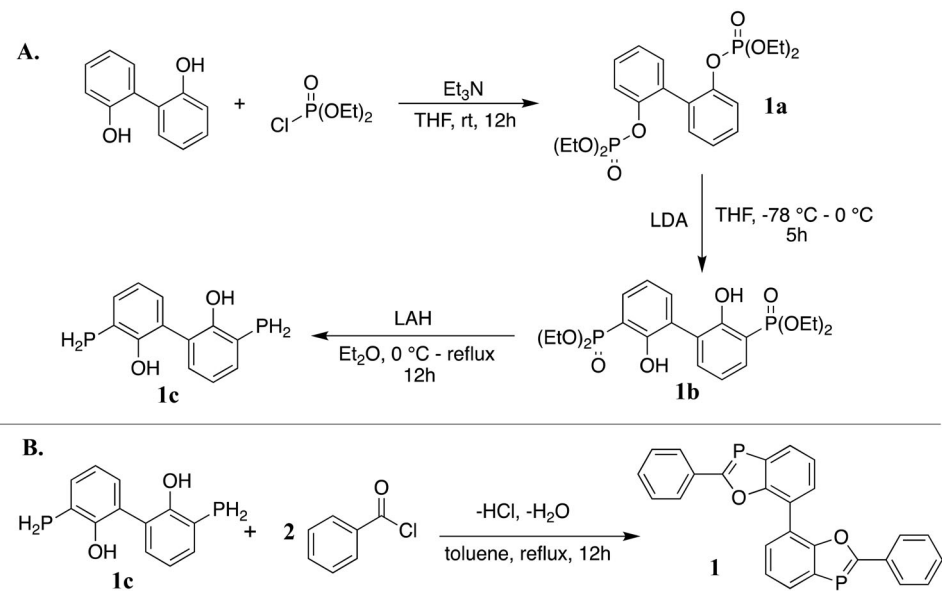
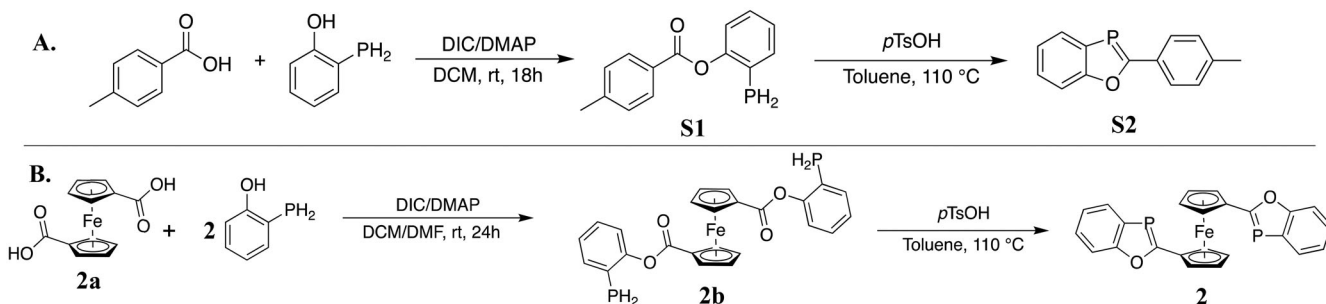


Figure 1. Selected examples of low-coordinate phosphorus containing heterocycles as “photo-copies.”



Scheme 1. (A) Preparation of diphosphine **1c**. (B) Synthesis of **1** via dehydrocyclization of **1c** with benzoyl chloride.



**Scheme 2.** (A) Model synthesis of 2-(4-MePh)BOP via Steglich esterification and dehydrocyclization. (B) Synthesis of 2 via Steglich esterification followed by dehydrocyclization with *p*TsOH.

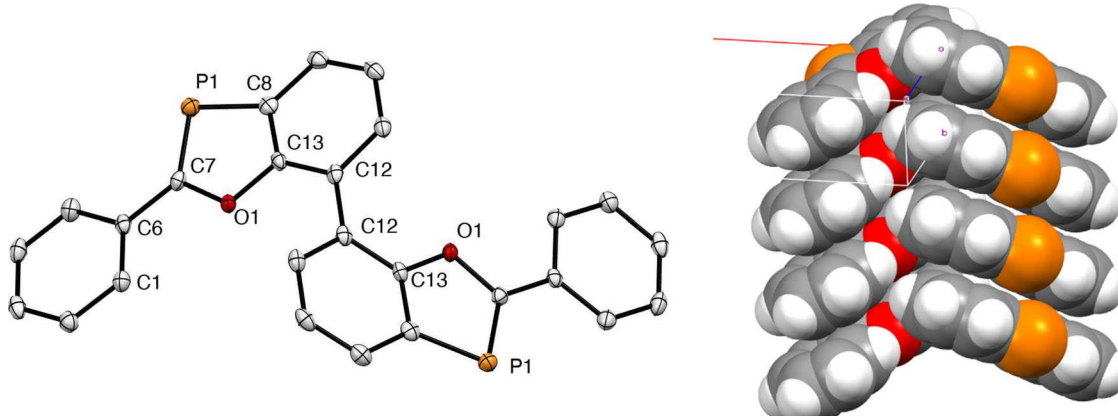


**Figure 2.** Structural (left) and packing (right) representations of 1. Hydrogen atoms omitted for clarity on left. Selected bond distances (Å) and angles (deg): P1-C7, 1.715(3); P1-C8, 1.790 (2); O1-C7, 1.378(3); C8-P1-C7, 88.4(1).

after workup as an analytically pure pale-yellow microcrystalline solid in 90% yield. Compound 1's solution properties are consistent with previously reported 2-Ar-BOPs. In solution, **1** displays bright blue fluorescence when irradiated at 365 nm. UV-vis measurements of **1** in THF show a max absorbance at  $\lambda_{\text{max}} = 336 \text{ nm}$ , and molar absorptivity of  $33,160 \text{ L}\cdot\text{mol}^{-1}\cdot\text{cm}^{-1}$ . The  $^{31}\text{P}\{^1\text{H}\}$  shift in  $\text{CDCl}_3$  appears at  $\delta + 86 \text{ ppm}$ , in line with other 2-Ar-BOPs (e.g., 2-(4-MePh)BOP,  $\delta + 83 \text{ ppm}$ ).<sup>[14]</sup>

Anchoring two BOPs to each ring of ferrocene should allow the BOP rings to remain parallel with respect to each other regardless of being conformationally *trans*- or eclipsed. Unlike synthesis of **1**, however, synthesis of a ferrocene linked bisBOP compound proved more complicated than expected. BOPs are typically prepared in one of two ways: 1.) condensation of 2-phosphinophenol with an imidoyl chloride,<sup>[14]</sup> or 2.) dehydrocyclization with an aryl acyl chloride.<sup>[21]</sup> In our hands, the reaction of 1,1'-ferrocenedicarbonyl chloride and 2-phosphinophenol yielded a mixture of unidentified products. The preparation of **2** gave an opportunity to develop a synthetic route new to the preparation of benzoxaphospholes. Specifically, the Steglich esterification, or carbodiimide coupling, was found to give conditions that productively and cleanly react with 2-phosphinophenol.

In a model reaction of 2-phosphinophenol and *p*-toluic acid, *N,N'*-diisopropylcarbodiimide (DIC) is a competent coupling agent in the preparation of the desired ester (**S1**)

shown in **Scheme 2A**. Purification via flash chromatography (silica gel 60, DCM) in ambient conditions affords **S1** as an oxygen and water stable primary phosphine. No phosphinoacetate coupling product was observed during this reaction. This suggests phosphorus has a comparatively low nucleophilicity compared to alcohols and primary amines under these conditions.

Coupling of 2-phosphinophenol with 1,1'-ferrocenedicarbonyl acid (**2a**) was met with additional challenges, as **2a** is relatively insoluble in DCM. Addition of 25% DMF in DCM aids in solubilizing **2a**. We found that this modification prepares the 2-phosphinophenylacetate (**2b**) (**Scheme 2B**) in satisfactory yield and purity. No reaction is observed upon heating the phenylacetate in toluene suggesting that dehydrocyclization in benzoxaphosphole syntheses are acid catalyzed. Addition of a catalytic amount of *p*-TsOH affords the bisBOP **2** as a brick red solid in a modest, unoptimized yield of 11% after flash chromatography. The  $^{31}\text{P}\{^1\text{H}\}$  NMR signal in  $\text{CDCl}_3$  for this compound appears at  $\delta + 79.77 \text{ ppm}$ , which is comparable to  $^{31}\text{P}$  NMR shifts for 2-*tert*-butyl and 2-adamantyl functionalized benzoxaphospholes.<sup>[14]</sup> The symmetry of the  $^1\text{H}$  NMR spectrum is consistent with the molecule freely rotating in solution on the NMR timescale.

### Solid state molecular structures

Crystals of **1** and **2** suitable for X-ray diffraction were grown from a saturated DCM solution cooled to  $-35^\circ\text{C}$  (**1**) or

slow cooling of a saturated toluene solution (**2**). The results of each study are portrayed in **Figures 2** and **3**, respectively.

The P=C bond length of 1.715 (3) Å, and C8–P1–C7 bond angle of 88.4(1)°, in **1** are in good agreement with the average bond lengths found in 2-aryl-BOPs.<sup>[14]</sup> For example, the corresponding values for 2-(4-chlorophenyl)-BOP are 1.712(2) Å and 88.15(9)° respectively.<sup>[22]</sup>

While 2-aryl-BOPs are generally planar molecules, the two BOPs in **1** are mutually not coplanar. The best plane of non-hydrogen atoms of each BOP is tilted by 47.8° from one another. The non-planarity of the two BOP units is reasonably attributed to steric clashes between the two hydrogen atoms nearest the oxygen atoms that would occur in the stretched out/flattened configuration. To explore this explanation in more detail, a series of DFT calculations (B3LYP/6-31G\*) were performed where the dihedral angle about the linking C12–C12' bond was systematically varied from 0 to

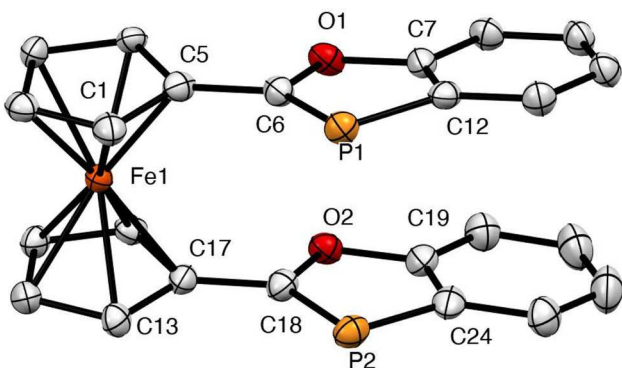


**Figure 3.** Structural diagram of **2**. Hydrogen atoms omitted for clarity. Selected bond distances (Å) and angles (deg): P1–C6, 1.700(6); P2–C18, 1.706(6); P1–C12, 1.808(6); P2–C24, 1.791(6); O1–C6, 1.364(6); O2–C18, 1.371(6); C6–P1–C12, 88.0(3); C18–P2–C24, 87.7(3). P1–C6–C5–C1, 12.59(9); P2–C18–C17–C13, 5.5(9).

180°. Two minima were located, one near 46° and the other around 128° (**Figure 4**). The former is consistent with the observed structure. The latter is most likely in facile equilibrium with the other conformation, as energy barrier is estimated to be small (*ca.* 1.5 kcal/mol). Qualitatively, the former conformer might be predicted to be better able to stack in the solid state as “cupped playing cards.” The packing diagram (**Figure 2**) shows this is indeed the preferred form with columns of both enantiomers of **1** aligning along the *b*-axis of the unit cell. The calculations also reveal that as the dihedral angle approaches 180°, the steric clashes between the 2-phenyl groups becomes severe and induces significant distortions in the BOP cores.

The solid-state structure of compound **2** is notably different from that displayed by **1**, in that the BOP entities are located just above and below each other (**Figure 3**). Centroid to centroid distances for the 5- and 6-membered rings of the BOP groups are 3.58 and 3.81 Å. Compared to centroid-to-centroid distance of the ferrocene linker (3.33 Å) there is some degree of  $\pi$ - $\pi$  repulsion between the BOP substituents. Interestingly, several other examples of ferrocene-linked heterocycles display this stacking arrangement, including a related example having two 2-phenyl-1,3-naphthoxazole units (centroid to centroid distance of 3.44 Å between oxazole rings).<sup>[23–26]</sup> In this example, however, the nitrogen atoms are pointed toward opposite directions (*anti*). To help explain this interesting orientation, an assessment of potential noncovalent interactions between the BOP groups in **2** was made via a DFT calculation (B3LYP/6-31G\*) and generation of a non-covalent interaction (NCI) plot shown in **Figure 5**.<sup>[27–29]</sup> The results do indeed suggest favorable attractions between the two BOP groups, as indicated by the green surfaces.

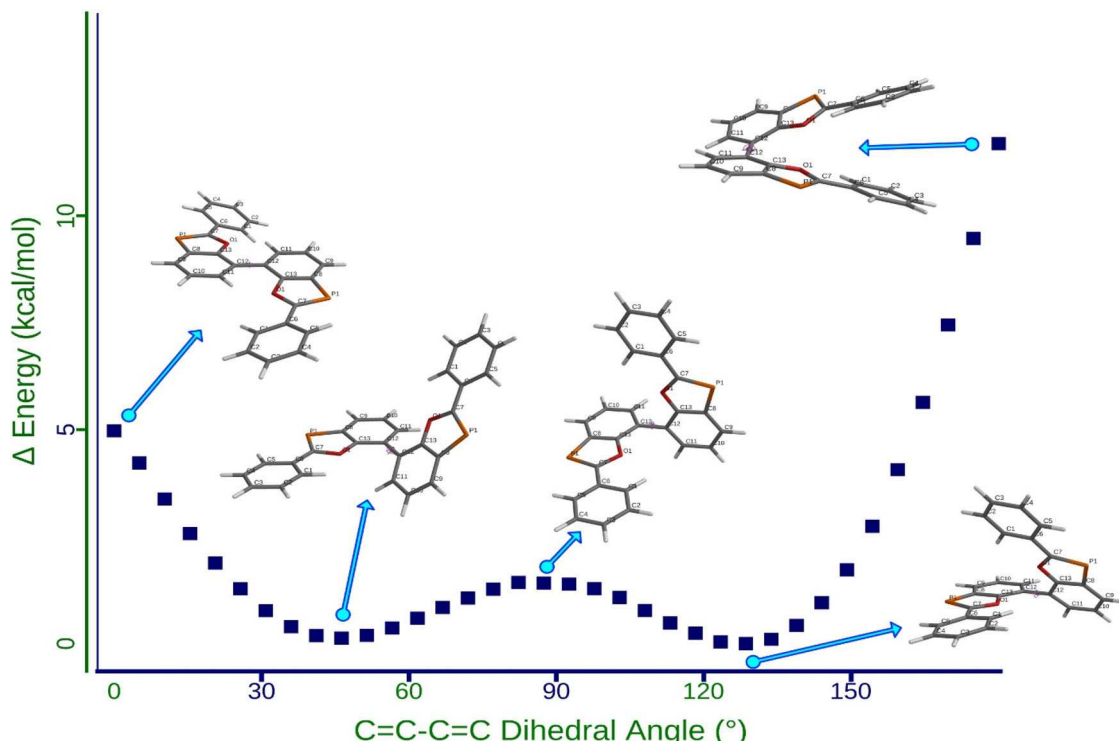


**Figure 4.** Plot of C12–C12' torsions from 0 to 180°, optimized at B3LYP/6-31G\*.

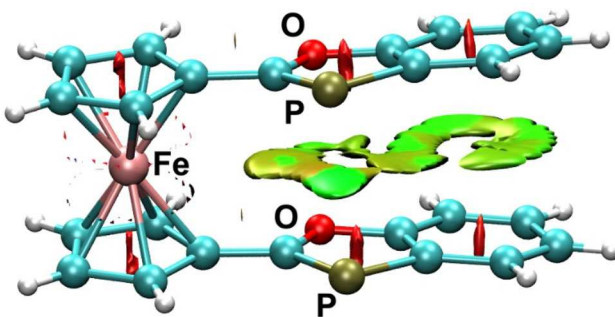


**Figure 5.** NCI plot of **2**. The green regions show weak attractive forces between the eclipsed BOP planes, red regions show repulsive interactions.

These observations are also consistent reports of 1,1'-bis-substituted ferrocenes which displaying an eclipsed conformation in the solid state, implying some benefit of intramolecular  $\pi$ - $\pi$  stacking combined with crystal packing forces.<sup>[30-38]</sup> In addition to the trans and eclipsed conformations, unsymmetric heterocycle rings may also adopt syn- and anti-conformations (in the case of BOPs, with respect to the P-atom).

The P1-C6 and P2-C18 bond lengths (1.700 and 1.706 Å, respectively) in **2** are on the short end of the average Aryl-BOP P=C bond (1.703–1.728 Å). Again, these metrics better resemble the 2-alkyl substituted BOPs.

### UV-visible and fluorescence

The colors of BOPs in the solid-state range anywhere from colorless to bright yellow. Compound **1**, which can be considered an electronically isolated pair of 2-Ar-BOPs, shares most optical properties common to many 2-Ar-BOPs. In the solid state, pale-yellow solid **1** displays no significant solid-state emission when irradiated with a handheld UV lamp. In solution, UV irradiation induces a vibrant blue emission. Absorbance and emission spectra of **1** in THF were collected over a range of concentrations. There is a single absorbance at 335 nm. The emission spectrum displays a single peak at 415 nm (THF, excitation at 366 nm). A plot of the  $\lambda_{\text{max}}$  versus concentration gives a linear trace with an  $R^2$  of 0.998 and the molar extinction coefficient was given to be  $33,200 \text{ M}^{-1} \cdot \text{cm}^{-1}$ , following Beer's law. The QY was measured to be 18% in THF, relative to quinine bisulfate and 9,10-diphenylanthracene. The Stokes shift of the emission is 79 nm, which is on the lower end of values observed for 2-Ar-BOP's (79–89 nm) (Figure 6).

Compound **2**, however, presents substantially different photophysical properties than **1** and most 2-Ar-BOPs. It is brick red in the solid state and in solution and displays no visible emission under 254 nm or 365 nm UV light in either state. The lack of emission from **2** is likely due to well-known emission quenching of fluorophores substituted with ferrocene.<sup>[34]</sup> In THF, the max absorbance peak appears at 326 nm with a shoulder near 357 nm. Additionally, there is a smaller absorbance at 490 nm. A plot of the  $\lambda_{\text{max}}$  versus concentration gives a linear trace with an  $R^2$  of 0.999 and the molar extinction coefficient was given to be  $24,500 \text{ M}^{-1} \cdot \text{cm}^{-1}$ , following Beer's law.

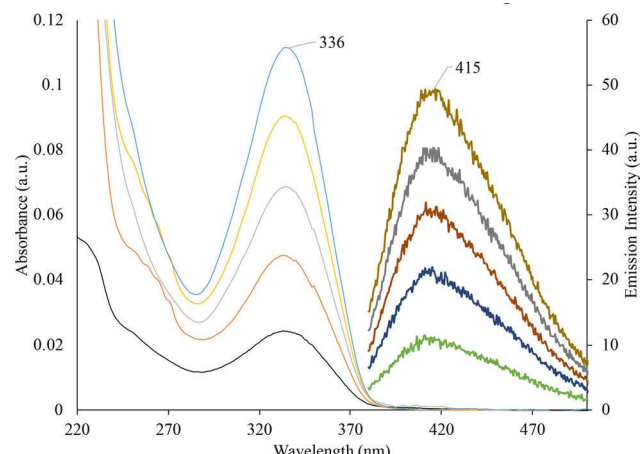


**Figure 6.** UV-vis absorbance and emission spectra of **1**.

### Conclusions

We have prepared and structurally characterized two non-planar bisBOPs. These examples act as proof of concept in generation of three-dimensional building block based on C=P bearing heterocycles. Further investigation into the application of these molecules as ligands, monomeric building blocks, and sensors is currently being explored. Analogues of compound **1** are primed for further studies of axially constrained bis(BOP) for CPL applications.<sup>[39,40]</sup> These compounds would be synthetically accessible because enantiomerically pure 2,2'-binaphthol is commercially available. While **2** lacks significant photoluminescence, further functionalization or metal ion binding might enhance this property.<sup>[41]</sup>

### Experimental

#### General synthetic methods

All oxygen and water sensitive materials were handled using standard Schlenk techniques under nitrogen or argon atmosphere or in a nitrogen filled MBraun glove box, unless otherwise specified. Toluene, methylene chloride, tetrahydrofuran and diethyl ether were supplied by an MBraun Solvent Purification System. Additional solvents were anhydrous ACS grade and used as received. Unless otherwise specified, all reagents and starting materials were used as received. Elemental Analysis was performed by Robertson Microlit Laboratories (Lewes, NJ). Preparation of 2-phosphino-phenol was conducted using a modified literature procedure.<sup>[42]</sup> 1,1'-ferrocenedicarboxylic acid (**2a**) was prepared as previously reported.<sup>[43]</sup>

#### NMR spectroscopy

NMR spectra were collected using a Bruker AVANCE III 500 or Varian Inova 400 spectrometer. Chemical shifts are internally referenced to residual solvent signals ( $^1\text{H}$  and  $^{13}\text{C}\{^1\text{H}\}$ ) or externally to 85%  $\text{H}_3\text{PO}_4$  ( $^{31}\text{P}\{^1\text{H}\}$ ).  $^{13}\text{C}$  and  $^{31}\text{P}$  NMR spectra were  $^1\text{H}$ -decoupled unless otherwise stated.

## Optical spectroscopy

Absorbance spectra were collected using a Cary 5000 spectrophotometer and are corrected for solvent background. Emission spectra were collected using a Cary Eclipse fluorescence spectrophotometer. All spectra were recorded at room temperature in 1.0 cm path length, screw top quartz cuvettes. All solutions were prepared under inert atmosphere with anhydrous degassed solvent, unless otherwise noted.

## Synthetic procedures

### [1,1'-biphenyl]-2,2'-diyl tetraethyl bis(phosphate) (1a)

A dry 100 mL Schlenk under argon was charged with 2,2'-biphenol (6.02 g, 32.3 mmol), and then evacuated and back-filled (3x) with argon 2,2'-biphenol was dissolved in anhydrous THF (40 mL), and then triethylamine (9.50 mL, 68.1 mmol) was added. To the colorless solution was added diethyl chlorophosphate (9.35 mL, 64.7 mmol), and the solution stirred at 50 °C for 24 hours. The mixture was cooled to ambient temperature, diluted with 50 mL of diethyl ether, and filtered. The filtrate was concentrated to an orange oil by rotary evaporation. The oil was dissolved in diethyl ether (60 mL) and washed with 1 M NaOH and brine followed by drying over sodium sulfate and magnesium sulfate. Removal of the diethyl ether by rotary evaporation and high vacuum led to a pale-yellow oil. Mass: 7.432 g (50%) <sup>1</sup>H NMR (500 MHz, CDCl<sub>3</sub>) δ 7.41 (d, *J* = 8.7 Hz, 2H), 7.30–7.32 (m, 4H), 7.18 (t, *J* = 7.3 Hz, 2H), 3.87 (h, *J* = 7.4 Hz, 8H), 1.14 (t, *J* = 7.1 Hz, 12H). <sup>31</sup>P{<sup>1</sup>H} NMR (203 MHz, CDCl<sub>3</sub>) δ = 8.9.

### Tetraethyl (2,2'-dihydroxy-[1,1'-biphenyl]-3,3'-diyl)bis(phosphonate) (1b)

A dry 200 mL Schlenk flask under argon was charged with *N,N'*-diisopropylamine (5.20 mL, 36.8 mmol) and THF (80 mL) and cooled to -78 °C. *n*-BuLi (15.0 mL, 2.48 M in hexanes, 37.2 mmol) was added dropwise via syringe and the solution was stirred for 2 hours yielding a yellow solution. To this mixture was added **1a** (7.43 g, 16.2 mmol) as a solution in THF (10 mL) dropwise via addition funnel. The mixture was stirred at -78 °C for 1 hour and for an additional 4 hours at 0 °C. The resulting beige slurry was quenched with 2 M HCl and stirred overnight. The mixture was transferred to a separatory funnel and the aqueous was extracted with diethyl ether (4 × 50 mL). The organic layers were combined, dried over sodium sulfate and magnesium sulfate before concentrating to a pale-yellow oil by rotary evaporation and high vacuum. Mass: 7.008 g (94%) <sup>1</sup>H NMR (400 MHz, CDCl<sub>3</sub>) δ 10.46 (s, 2H), 7.54 (ddd, *J* = 7.5, 1.8, 0.9 Hz, 2H), 7.41 (ddd, *J* = 14.3, 7.7, 1.8 Hz, 2H), 7.00 (td, *J* = 7.6, 3.5 Hz, 2H), 4.28–4.00 (m, 8H), 1.34 (td, *J* = 7.0, 0.7 Hz, 12H). <sup>31</sup>P{<sup>1</sup>H} NMR (162 MHz, CDCl<sub>3</sub>) δ 23.7.

### 3,3'-Bis(phosphino)-[1,1'-biphenyl]-2,2'-diol (1c)

A dry 250 mL 2-neck round bottom flask and reflux condenser under argon was charged with LiAlH<sub>4</sub> (3.46 g,

91.2 mmol), cooled to 0 °C. Diethyl ether (100 mL) was added, followed by dropwise addition of a solution of **1b** (7.0 g, 15.3 mmol) in THF (10 mL), taking care to excessive reaction. The flask was then heated at reflux for 6 hours. The mixture was cooled to 0 °C and remaining LiAlH<sub>4</sub> was quenched by slow addition of argon-purged water (100 mL). The mixture was acidified using concentrated HCl and stirred. The contents were transferred to a separatory funnel under argon and the organic portion reserved. The aqueous was extracted with additional diethyl ether (2 × 50 mL) and the organic layers were combined. Pyridine (1.2 mL) was added and stirred for 15 minutes. The mixture was washed with 2 M HCl (50 mL, argon-purged) and then dried over sodium sulfate and magnesium sulfate, filtered, and concentrated under reduced pressure. The resulting colorless oil crystallized upon standing overnight. Colorless solid: 3.20 g (87%) <sup>1</sup>H NMR (500 MHz, CDCl<sub>3</sub>) δ 7.53 (t, *J* = 7.6 Hz, 2H), 7.23 (d, *J* = 7.5 Hz, 2H), 6.99 (t, *J* = 7.6 Hz, 2H), 5.68 (s, 2H), 3.88 (d, *J* = 206.3 Hz, 4H). <sup>31</sup>P{<sup>1</sup>H} NMR (203 MHz, CDCl<sub>3</sub>) δ = 145.2. <sup>31</sup>P NMR (203 MHz, CDCl<sub>3</sub>) δ = 145.2 (t, *J<sub>PH</sub>* = 206.5 Hz).

### 2,2'-Diphenyl-7,7'-bibenzo[d][1,3]benzoxaphosphole (1)

A dry 100 mL Schlenk flask was charged with benzoyl chloride (1.55 mL, 13.3 mmol) and toluene (50 mL) under argon. To this mixture was added a solution of **1c** (1.68 g, 6.6 mmol) in toluene (10 mL). The reaction was stirred for 1 hour before heating at 70 °C under argon overnight. A ring of yellow crystalline solid and water condensation inside the flask was visible. The flask was fitted with a Dean-Stark apparatus and purged with argon for 5 minutes. The water was azeotropically distilled to 1/2 volume using a Dean-Stark apparatus with heating in a 170 °C oil bath. The solution was cooled, during which a pale-yellow crystalline solid precipitated. A sample was taken to collect <sup>1</sup>H and <sup>31</sup>P{<sup>1</sup>H} NMR, which showed nearly quantitative conversion. The solid was dried overnight under high vacuum before storing in a glove box. Pale yellow solid: 2.80 g (90%) after trituration with anhydrous DCM. NMR (500 MHz, CDCl<sub>3</sub>) δ 8.09 (dd, *J* = 7.1, 2.8 Hz, 2H), 7.84–7.74 (m, 6H), 7.48 (td, *J* = 7.5, 2.1 Hz, 2H), 7.25 (d, *J* = 3.6 Hz, 6H). <sup>31</sup>P{<sup>1</sup>H} NMR (203 MHz, CDCl<sub>3</sub>) δ 86.0. <sup>13</sup>C NMR (126 MHz, CDCl<sub>3</sub>) δ 197.1 (d, *J<sub>PC</sub>* = 55.3 Hz), 157.3 (d, *J<sub>PC</sub>* = 4.3 Hz), 137.8, 137.5, 134.5 (d, *J<sub>PC</sub>* = 12.9 Hz), 129.9 (d, *J<sub>PC</sub>* = 4.6 Hz), 129.2 (d, *J<sub>PC</sub>* = 20.3 Hz), 128.9, 128.9, 128.9, 124.9 (d, *J<sub>PC</sub>* = 14.1 Hz), 123.6 (d, *J<sub>PC</sub>* = 10.0 Hz), 123.5. Anal. Calcd for C<sub>26</sub>H<sub>16</sub>O<sub>2</sub>P<sub>2</sub>: C, 73.94; H, 3.82. Found: C, 74.20; H, 3.59. UV (THF):  $\lambda_{\text{max}}$ , nm ( $\epsilon$ , M<sup>-1</sup> cm<sup>-1</sup>) 336 (33,200). Fluorescence (THF):  $\lambda_{\text{ex}}$ , 366 nm,  $\lambda_{\text{em}}$ , 415 nm. Quantum Yield (THF):  $\Phi$  0.18

### 1,1'-Bis(2-phosphinophenoxy carbonyl)ferrocene (2b)

A dry 50 mL Schlenk flask was charged with 1,1'-ferrocene dicarboxylic acid (0.547 g, 1.99 mmol), 2-phosphinophenol (0.530 g, 4.20 mmol) and DMAP (0.247 g, 2.02 mmol) before

dissolving in 20 mL of a DCM/DMF solvent mixture (3:1). The flask was sealed with a septum and filled with before adding *N*-*N*'-diisopropylcarbodiimide (0.650 mL, 4.15 mmol) in one portion. This orange solution was left to stir at RT overnight. The solution was concentrated under high vacuum, and the damp orange solid was dissolved in 50 mL of degassed DCM. This solution was washed sequentially with 25 mL of saturated sodium bicarbonate, 1 M NaOH, and 2 M HCl, before drying over anhydrous sodium sulfate. The resulting diphosphine was filtered through a pad of silica gel, eluting with DCM. The first red eluent was collected and concentrated to yield an orange solid which was used in next step without further purification.  $^1\text{H}$  NMR (500 MHz, DMSO)  $\delta$  7.62 (t,  $J$  = 7.0 Hz, 2H), 7.39 (t,  $J$  = 7.8 Hz, 2H), 7.28 (d,  $J$  = 8.2 Hz, 2H), 7.23 (t,  $J$  = 7.4 Hz, 2H), 5.12 (s, 4H), 4.84 (s, 4H), 3.87 (d,  $J$  = 208.1 Hz, 4H).  $^{31}\text{P}$  NMR (203 MHz, DMSO)  $\delta$  = 138.7 (t,  $J_{\text{PH}}$  = 207.9 Hz).

### 1,1'-Bis(2-benzo[d][1,3]oxaphosphole)ferrocene (2)

Freshly prepared diphosphine **2b** (as described above) was transferred to a dry 50 mL Schlenk flask under argon and dissolved in toluene (25 mL). To this was added *p*-TsOH (10 mol%) before sealing with a septum under a static argon supply. The mixture was heated in a 120 °C oil bath overnight, during which a color change from orange to brick-red was observed. The reaction mixture was cooled and concentrated before filtering through a plug of silica gel (*ca.* 1"  $\times$  1") eluting with DCM. The first red color band was isolated, giving **2** as a brick red solid. Mass 0.100 g (11%, based on **2a**).  $^1\text{H}$  NMR (400 MHz,  $\text{CDCl}_3$ )  $\delta$  7.58 (d,  $J$  = 7.61 Hz, 2H), 7.21–7.10 (m, 4H), 7.02 (d,  $J$  = 7.53 Hz, 2H), 4.79 (t,  $J$  = 1.9 Hz, 4H), 4.45 (t,  $J$  = 1.8 Hz, 4H).  $^{31}\text{P}\{\text{H}\}$  NMR (203 MHz,  $\text{CDCl}_3$ )  $\delta$  79.8.  $^{13}\text{C}$  NMR (126 MHz,  $\text{CDCl}_3$ )  $\delta$  193.0 (d,  $J_{\text{PC}}$  = 53.0 Hz), 159.5, 136.7–136.0 (m), 128.6 (dt,  $J_{\text{PC}}$  = 18.8, 8.8 Hz), 126.2, 122.5 (t,  $J_{\text{PC}}$  = 4.9 Hz), 112.7, 82.5–81.9 (m), 71.7, 68.1 (t,  $J_{\text{PC}}$  = 4.0 Hz). Anal. Calcd for  $\text{C}_{24}\text{H}_{16}\text{FeO}_2\text{P}_2$ : C, 63.47; H, 3.55. Found: C, 63.52; H, 3.26. UV (THF):  $\lambda_{\text{max}}$ , nm ( $\epsilon$ ,  $\text{M}^{-1}\text{cm}^{-1}$ ) 326 (24,500).

### Associated content

#### Supporting information

Computational details, crystallographic information, and additional UV-visible/emission data (PDF).

#### Accession codes

CCDC 2119420–2119421 contain the supplementary crystallographic data for this paper. These data can be obtained free of charge via [www.ccdc.cam.ac.uk/data\\_request/cif](http://www.ccdc.cam.ac.uk/data_request/cif), or by emailing [data\\_request@ccdc.cam.ac.uk](mailto:data_request@ccdc.cam.ac.uk), or by contacting The Cambridge Crystallographic Centre, 12 Union Road, Cambridge CB2 1EZ, UK; fax +44 1223 336033.

### Disclosure statement

The authors declare no competing financial interests.

### Funding

This work was supported by the National Science Foundation (CHE #1955845).

### ORCID

Zakary T. Ekstrom  <http://orcid.org/0000-0002-8069-4895>  
 Arnold L. Rheingold  <http://orcid.org/0000-0003-4472-8127>  
 John D. Protasiewicz  <http://orcid.org/0000-0002-3332-6985>

### References

- [1] Bates, J. I.; Dugal-Tessier, J.; Gates, D. P. Phospha-Organic Chemistry: From Molecules to Polymers. *Dalt. Trans.* **2010**, 39, 3151–3159. DOI: [10.1039/B918938F](https://doi.org/10.1039/B918938F).
- [2] Hissler, M.; Lescop, C.; Réau, R. Functional Phosphorus-Based  $\pi$ -Conjugated Systems: Structural Diversity without Multistep Synthesis. *Pure Appl. Chem.* **2007**, 79, 201–212. DOI: [10.1351/pac200779020201](https://doi.org/10.1351/pac200779020201).
- [3] Pfeifer, G.; Chahdoura, F.; Papke, M.; Weber, M.; Szűcs, R.; Geffroy, B.; Tondelier, D.; Nyulászi, L.; Hissler, M.; Müller, C. Synthesis, Electronic Properties and OLED Devices of Chromophores Based on  $\lambda$  5 -Phosphinines. *Chem. Eur. J.* **2020**, 26, 10534–10543. DOI: [10.1002/chem.202000932](https://doi.org/10.1002/chem.202000932).
- [4] Hirai, M.; Tanaka, N.; Sakai, M.; Yamaguchi, S. Structurally Constrained Boron-, Nitrogen-, Silicon-, and Phosphorus-Centered Polycyclic  $\pi$ -Conjugated Systems. *Chem. Rev.* **2019**, 119, 8291–8331.
- [5] Baumgartner, T.; Réau, R. Organophosphorus  $\pi$ -Conjugated Materials. *Chem. Rev.* **2006**, 106, 4681–4727.
- [6] Chen, H.; Delaunay, W.; Yu, L.; Joly, D.; Wang, Z.; Li, J.; Wang, Z.; Lescop, C.; Tondelier, D.; Geffroy, B.; et al. 2,2'-Biphospholes: Building Blocks for Tuning the HOMO-LUMO Gap of  $\pi$ -Systems Using Covalent Bonding and Metal Coordination. *Angew. Chem. Int. Ed. Engl.* **2012**, 51, 214–217. DOI: [10.1002/anie.201105924](https://doi.org/10.1002/anie.201105924).
- [7] Simpson, M. C.; Protasiewicz, J. D. Phosphorus as a Carbon Copy and as a Photocopy: New Conjugated Materials Featuring Multiply Bonded Phosphorus. *Pure Appl. Chem.* **2013**, 85, 801–815. DOI: [10.1351/PAC-CON-12-09-13](https://doi.org/10.1351/PAC-CON-12-09-13).
- [8] Karabunarliev, S.; Baumgarten, M.; Tyutulyukov, N.; Muellen, K. Structure and Optical Absorption of Oligo(*p*- and *m*-Phenylenavinylenes) and Their Radical Anions: A Comparative Theoretical Study. *J. Phys. Chem.* **1994**, 98, 11892–11901. DOI: [10.1021/j100097a015](https://doi.org/10.1021/j100097a015).
- [9] Mathey, F. Phospha-Organic Chemistry: Panorama and Perspectives. *Angew. Chem. Int. Ed. Engl.* **2003**, 42, 1578–1604.
- [10] Priegert, A. M.; Rawe, B. W.; Serin, S. C.; Gates, D. P. Polymers and the P-Block Elements. *Chem. Soc. Rev.* **2016**, 45, 922–953.
- [11] Mathey, F. Expanding the Analogy between Phosphorus-Carbon and Carbon-Carbon Double Bonds. *Acc. Chem. Res.* **1992**, 25, 90–96. DOI: [10.1021/ar00014a006](https://doi.org/10.1021/ar00014a006).
- [12] Wu, S.; Rheingold, A. L.; Golen, J. A.; Grimm, A. B.; Protasiewicz, J. D. Synthesis of a Luminescent Azaphosphole. *Eur. J. Inorg. Chem.* **2016**, 2016, 768–773. DOI: [10.1002/ejic.201501279](https://doi.org/10.1002/ejic.201501279).
- [13] Worch, J. C.; Chirdon, D. N.; Maurer, A. B.; Qiu, Y.; Geib, S. J.; Bernhard, S.; Noonan, K. J. T. Synthetic Tuning of Electronic and Photophysical Properties of 2-Aryl-1,3-Benzothiaphospholes. *J. Org. Chem.* **2013**, 78, 7462–7469.
- [14] Washington, M. P.; Gudimetla, V. B.; Laughlin, F. L.; Deligonul, N.; He, S.; Payton, J. L.; Simpson, M. C.;

Protasiewicz, J. D. Phosphorus Can Also Be a “Photocopy.” *J. Am. Chem. Soc.* **2010**, *132*, 4566–4567. DOI: [10.1021/ja1009426](https://doi.org/10.1021/ja1009426).

[15] Ito, S.; Koshino, K.; Mikami, K. CF<sub>3</sub>-Inspired Synthesis of Air-Tolerant 9-Phosphoanthracenes That Feature Fluorescence and Crystalline Polymorphs. *Chem. Asian J.* **2018**, *13*, 830–837. DOI: [10.1002/asia.201701669](https://doi.org/10.1002/asia.201701669).

[16] Sklorz, J. A. W.; Hoof, S.; Rades, N.; De Rycke, N.; Könczöl, L.; Szieberth, D.; Weber, M.; Wiecko, J.; Nyulászi, L.; Hissler, M.; Müller, C. Pyridyl-Functionalised <sup>3</sup>H-1,2,3,4-Triazaphospholes: Synthesis, Coordination Chemistry and Photophysical Properties of Low-Coordinate Phosphorus Compounds. *Chem. Eur. J.* **2015**, *21*, 11096–11109. DOI: [10.1002/chem.201500988](https://doi.org/10.1002/chem.201500988).

[17] Nagahora, N.; Goto, S.; Inatomi, T.; Tokumaru, H.; Matsubara, K.; Shioji, K.; Okuma, K. Buchwald–Hartwig Amination of Phosphinines and the Effect of Amine Substituents on Optoelectronic Properties of the Resulting Coupling Products. *J. Org. Chem.* **2018**, *83*, 6373–6381.

[18] Qiu, Y.; Worch, J. C.; Chirdon, D. N.; Kaur, A.; Maurer, A. B.; Amsterdam, S.; Collins, C. R.; Pintauer, T.; Yaron, D.; Bernhard, S.; Noonan, K. J. T. Tuning Thiophene with Phosphorus: Synthesis and Electronic Properties of Benzobisthiaphospholes. *Chem. Eur. J.* **2014**, *20*, 7746–7751. DOI: [10.1002/chem.201402561](https://doi.org/10.1002/chem.201402561).

[19] Wu, S.; Rheingold, A. L.; Protasiewicz, J. D. Luminescent Materials Containing Multiple Benzoxaphosphole Units. *Chem. Commun. (Camb.)* **2014**, *50*, 11036–11038.

[20] Ndimba, A.; Roisnel, T.; Argouarch, G.; Lalli, C. Harvesting New Chiral Phosphotriesters by Phosphorylation of BINOL and Parent Bis-Phenols. *Synthesis (Stuttg.)* **2019**, *51*, 865–873.

[21] Grimm, A. B.; Wang, K.; Rheingold, A. L.; Moore, C. E.; Szieberth, D.; Nyulászi, L.; Protasiewicz, J. D. 2-Aryl-1,3-Benzoxaphospholes as Unwilling Participants for Catalytic Suzuki–Miyaura CC Coupling Reactions. *Organometallics* **2021**, *40*, 3436–3444. DOI: [10.1021/acs.organomet.1c00462](https://doi.org/10.1021/acs.organomet.1c00462).

[22] Hausen, H.-D.; Weckler, G. 2-p-Chlorophenyl-1,3-benzoxaphosphol Molekül- und Kristallstruktur eines  $\sigma^2$ -P=C—O-Derivates. *Z. anorg. allg. Chem.* **1985**, *520*, 107–112. DOI: [10.1002/zaac.19855200114](https://doi.org/10.1002/zaac.19855200114).

[23] Li, H.; Wei, K.; Wu, Y.-J. A Convenient Synthesis of 2-Arylnaphtho[1,2-d]Oxazole Derivatives Promoted by Triethylamine. *Chin. J. Chem.* **2007**, *25*, 1704–1709. DOI: [10.1002/cjoc.200790315](https://doi.org/10.1002/cjoc.200790315).

[24] Baumgardt, I.; Butenschön, H. 1,1'-Diaryl-Substituted Ferrocenes: Up to Three Hinges in Oligophenylenethynylene-Type Molecular Wires. *Eur. J. Org. Chem.* **2010**, *2010*, 1076–1087. DOI: [10.1002/ejoc.200901252](https://doi.org/10.1002/ejoc.200901252).

[25] Ogawa, S.; Kobayashi, H.; Muraoka, H. Synthesis, Structure, and Redox Properties of 1,1'-Bis(Aryloligothienyl)Ferrocenes. *Phosphorus Sulfur Silicon Relat. Elem.* **2011**, *186*, 1238–1245. DOI: [10.1080/10426507.2010.524178](https://doi.org/10.1080/10426507.2010.524178).

[26] Luo, Q.; Zhang, R.; Zhang, J.; Xia, J. Synthesis of Conjugated Main-Chain Ferrocene-Containing Polymers through Melt-State Polymerization. *Organometallics* **2019**, *38*, 2972–2978. DOI: [10.1021/acs.organomet.9b00312](https://doi.org/10.1021/acs.organomet.9b00312).

[27] Johnson, E. R.; Keinan, S.; Mori-Sánchez, P.; Contreras-García, J.; Cohen, A. J.; Yang, W. Revealing Noncovalent Interactions. *J. Am. Chem. Soc.* **2010**, *132*, 6498–6506.

[28] Lu, T.; Chen, F. Multiwfn: A Multifunctional Wavefunction Analyzer. *J. Comput. Chem.* **2012**, *33*, 580–592.

[29] Humphrey, W.; Dalke, A.; Schulten, K. VMD: Visual Molecular Dynamics. *J. Mol. Graph.* **1996**, *14*, 33–38.

[30] Blanchard, M. D.; Hughes, R. P.; Concolino, T. E.; Rheingold, A. L.  $\pi$ -Stacking between Pentafluorophenyl and Phenyl Groups as a Controlling Feature of Intra- and Intermolecular Crystal Structure Motifs in Substituted Ferrocenes. Observation of Unexpected Face-to-Face Stacking between Pentafluorophenyl Rings. *Chem. Mater.* **2000**, *12*, 1604–1610. DOI: [10.1021/cm000093j](https://doi.org/10.1021/cm000093j).

[31] Mata, J. A.; Peris, E.; Llusr, R.; Uriel, S.; Cifuentes, M. P.; Humphrey, M. G.; Samoc, M.; Luther-Davies, B. Syntheses, Structures and Nonlinear Optical Properties of Ferrocenyl Complexes with Arylethenyl Substituents. *Eur. J. Inorg. Chem.* **2001**, *2001*, 2113–2122. DOI: [10.1002/1099-0682\(200108\)2001:8<2113::AID-EJIC2113>3.0.CO;2-1](https://doi.org/10.1002/1099-0682(200108)2001:8<2113::AID-EJIC2113>3.0.CO;2-1).

[32] Enders, M.; Kohl, G.; Pritzkow, H. Synthesis and Coordination Behaviour of the New (8-Quinolyl)Cyclopentadienyl Ligand. *J. Organomet. Chem.* **2001**, *622*, 66–73. DOI: [10.1016/S0022-328X\(00\)00866-4](https://doi.org/10.1016/S0022-328X(00)00866-4).

[33] Anderson, J. C.; White, C.; Stenson, K. P. Synthesis of Ferrocene Bridged Bis (2-Indenyl) Ligands. *Synlett* **2002**, *2002*, 1511–1513. DOI: [10.1055/s-2002-33524](https://doi.org/10.1055/s-2002-33524).

[34] Fery-Forgues, S.; Delavaux-Nicot, B. Ferrocene and Ferrocenyl Derivatives in Luminescent Systems. *J. Photochem. Photobiol. A Chem.* **2000**, *132*, 137–159. DOI: [10.1016/S1010-6030\(00\)00213-6](https://doi.org/10.1016/S1010-6030(00)00213-6).

[35] Donoli, A.; Bisello, A.; Cardena, R.; Crisma, M.; Orian, L.; Santi, S. Charge Transfer Properties of Benzo [b] Thiophene Ferrocenyl Complexes. *Organometallics* **2015**, *34*, 4451–4463. DOI: [10.1021/acs.organomet.5b00191](https://doi.org/10.1021/acs.organomet.5b00191).

[36] Lima, C. F. R. A. C.; Fernandes, A. M.; Melo, A.; Gonçalves, L. M.; Silva, A. M. S.; Santos, L. M. N. B. F. Diarylferrocene Tweezers for Cation Binding. *Phys. Chem. Chem. Phys.* **2015**, *17*, 23917–23923.

[37] Sivaev, I. Ferrocene and Transition Metal Bis(Dicarbollides) as Platform for Design of Rotatory Molecular Switches. *Molecules* **2017**, *22*, 2201. DOI: [10.3390/molecules2212201](https://doi.org/10.3390/molecules2212201).

[38] Takai, A.; Yasuda, T.; Ishizuka, T.; Kojima, T.; Takeuchi, M. A Directly Linked Ferrocene-Naphthalenediimide Conjugate: Precise Control of Stacking Structures of  $\pi$ -Systems by Redox Stimuli. *Angew. Chem. Int. Ed. Engl.* **2013**, *52*, 9167–9171. DOI: [10.1002/anie.201302587](https://doi.org/10.1002/anie.201302587).

[39] Maniappan, S.; Jadhav, A. B.; Kumar, J. Template Assisted Generation of Chiral Luminescence in Organic Fluorophores. *Front. Chem.* **2021**, *8*, 1–7. DOI: [10.3389/fchem.2020.557650](https://doi.org/10.3389/fchem.2020.557650).

[40] Kumar, J.; Nakashima, T.; Kawai, T. Circularly Polarized Luminescence in Chiral Molecules and Supramolecular Assemblies. *J. Phys. Chem. Lett.* **2015**, *6*, 3445–3452.

[41] Zapata, F.; Caballero, A.; Espinosa, A.; Tárraga, A.; Molina, P. Imidazole-Annelated Ferrocene Derivatives as Highly Selective and Sensitive Multichannel Chemical Probes for Pb(II) Cations. *J. Org. Chem.* **2009**, *74*, 4787–4796.

[42] Couillens, X.; Gressier, M.; Coulais, Y.; Dartiguenave, M. Synthesis and Physicochemical Characterization of Oxo and Phenylimido Re(V), Re(III) and Ni(II) Complexes with the 2-[Bis(Ethoxyethyl)Phosphino]Phenolato Ligand and Derivatives. *Inorganica Chim. Acta* **2004**, *357*, 195–201. DOI: [10.1016/S0020-1693\(03\)00388-8](https://doi.org/10.1016/S0020-1693(03)00388-8).

[43] Gao, B.; Yang, B.; Li, T.; Zhang, B. Synthesis and Characterization of Ester Ferrocenophanes. *Synth. Commun.* **2009**, *39*, 2973–2981. DOI: [10.1080/00397910802716150](https://doi.org/10.1080/00397910802716150).